IFASD 2015
International Forum on Aeroelasticity and Structural Dynamics
June 28 — July 02, 2015 ▲ Saint Petersburg, Russia

The Aeroelastic Impact of Engine Thrust and Gyroscopics on Aircraft Flutter Instabilities

Stefan Waitz [1], Holger Hennings [1]

[1] Institute of Aeroelasticity, DLR, Göttingen, Germany

stefan.waitz@dlr.de, holger.hennings@dlr.de

Keywords: Flutter, gyroscopics, engine thrust, follower force, asymmetric eigenmode, engine aeroelasticity, critical speed, flutter frequency, aerodynamic damping

Abstract

Since more and more modern civil aircraft are equipped with UHBR-engines for reasons of fuel efficiency and environmental aspects, the need to tackle specific engine related dynamic problems has occurred. The request for UHBR-engines with high bypass ratio numbers and with their intrinsic advantages of economic fuel consumption and lower acoustic emission asks for enhanced vibration prediction capabilities. Beside the energetic benefits such engines add to the aircraft design their rotating large diameter fans can influence the dynamic behaviour of the complete elastic aircraft fuselage in a very unfavourable manner. Additional questions which arise with regard to structural dynamics and aeroelastic stability are treated in this work.

Especially in the scenario when large rotating engine masses are to be combined with elastic wing structures the possible occurrence of specific structural vibration problems can be avoided by taking the gyroscopic effects into account. As another important engine related aspect the modelling and the impact of the engine thrust is highlighted by integrating the first order deformation induced terms into the dynamical simulation model.

By introducing an increased coupling level between the degrees of freedom in the equation of motion (through additional off-diagonal terms) both eigenfrequencies and eigenmodes are affected. In the case of high engine participation in the structural deformation we can observe a lowering of the eigenfrequencies (in the test aeroplane up to 6[%]) and a loss in symmetry properties in the now strongly asymmetric eigenmodes. With the occurrence of flutter cases the critical speed had been experienced to shift about an amount of similar magnitude. Although in the presented cases the flutter speed moved to higher values, it was found indespensable to check every individual aircraft configuration with regard to the stability margin.

1 INTRODUCTION

The dynamic behaviour of an aeroplane with regard to aeroelastics is defined fundamentally by the movement of its elastically deformable aerodynamic surfaces. Together with the lift producing wings the components of the empennage (HTP, VTP) play a decisive role concerning the aeroelastic stability of an aeroplane and the possible occurrence of flutter and critical flight speeds. A physically quite different phenomenon in connection with the flutter behaviour emanates from the aircraft engines when providing the necessary thrust in flight. The rotatory masses of the different engine sections exert a specific influence on the elastic vibrations of the aircraft structure which can be compared to the gyroscopic behaviour caused by a gyrostat moment. This can be incorporated also into the stability formulation of the linearized equations of motion. As the solution of the eigenvalue problem shows the spin of the engine rotors causes a clear phase shift between the movement of the nacelle and e.g. the adjacent wing structure, thus yielding totally complex eigenmodes even for the vacuum modes. In general the movement of the gyrostat breaks the symmetry of the aircraft structure and leads to a coupling of the symmetric and antimetric eigenmodes which results in an asymmetric body motion. Along with the gyroscopics the thrust of the engines imposed on the bearing wing structure can play another destabilizing role in the aeroelastic balance. In the shape of follower forces the thrust related terms of the linearized deformed state are introduced into the equations of motion.

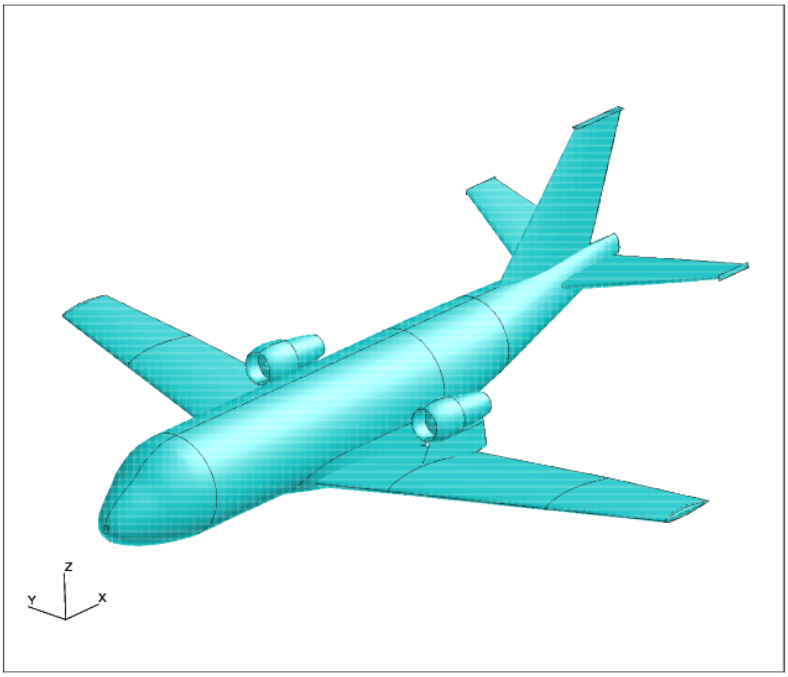

Figure 1: Scheme of the investigated aircraft VFW–614 ATTAS

Furthermore the corresponding flutter state depends on the distribution of the engine mass (c/g position) and pylon stiffness together with the kinematic attachment characteristics. The engines of the investigated aircraft type have a rearward position on the upper side of the wings which justifies the assumption of a quite considerable influence on the flutter behaviour of the overall aeroplane. This investigation is focused on the impact of the engines in operation on the global stability behaviour of an aeroplane which generally

can have either a damping or an exciting character thus resulting in a lift or a lowering of the critical flight speed. Therefore it should be conducted for every specific wing/engine or fuselage/engine configuration. The numerical simulation model of the respective case must be expanded by the so called terms of second order.

2 THE INVESTIGATED AIRPLANE MODEL BUILD-UP

The aeroplane investigated in this research work has been a VFW-614. Designed and built in the sixties of the 20^{th} century in Germany, the VFW-614 ATTAS served as a multiple purpose research platform in the DLR fleet until the end of 2012. Motivated by prior investigations of generic aeroplane models the main reason for choosing the VFW-614 ATTAS was its specific engine/wing configuration (see Fig.1). The engines are mounted on pylons which are placed on the upper side of the wings in the rearward part near the trailing edges. The flutter behaviour is presumably sensitive to this specific engine placement on the wing and therefore it was considered worthwile to submit the flutter analysis of this configuration (and the respective equations of motion) to a model extension by the engine related terms in focus.

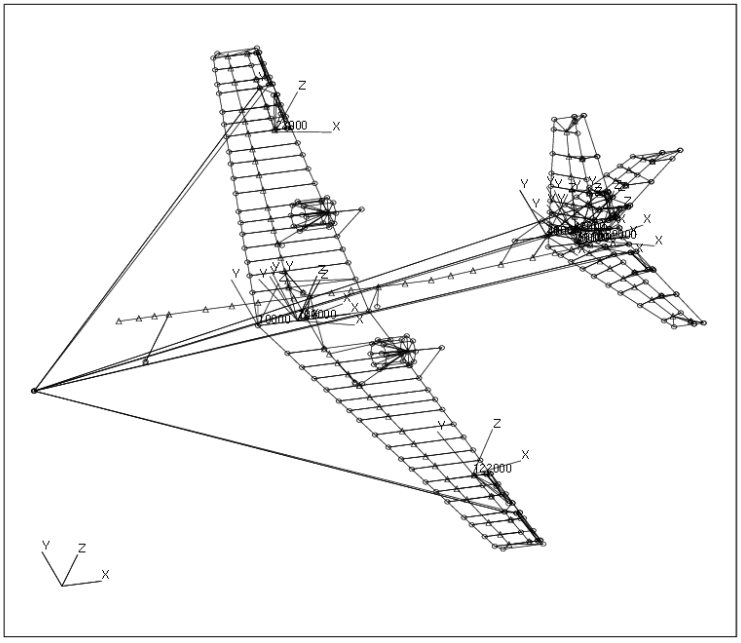

Figure 2: FEM beam model of the investigated aircraft VFW–614 ATTAS

The structural part of the aeroplane was built up by a FEM stick model where fuselage, wings and empennage were composed by about 100 beam elements (see Fig.2), with approximately 600 degrees of freedom comprising the A-SET of the solver. Within the commercial code NASTRAN (SOL 103) the eigenvalue solution of the discretized linear equations of motion rendered the necessary set of eigenfrequencies and eigenshapes. Out of this set the first 50 modes, including the six zero frequency rigid body motion shapes (see Tab.1), had been extracted and imported into the flutter solver for further use. The commercial code ZAERO then had been applied for both the build-up of the aerodynamic part of the aeroplane model and the solving of the complete aeroelastic equation of motion in the frequency

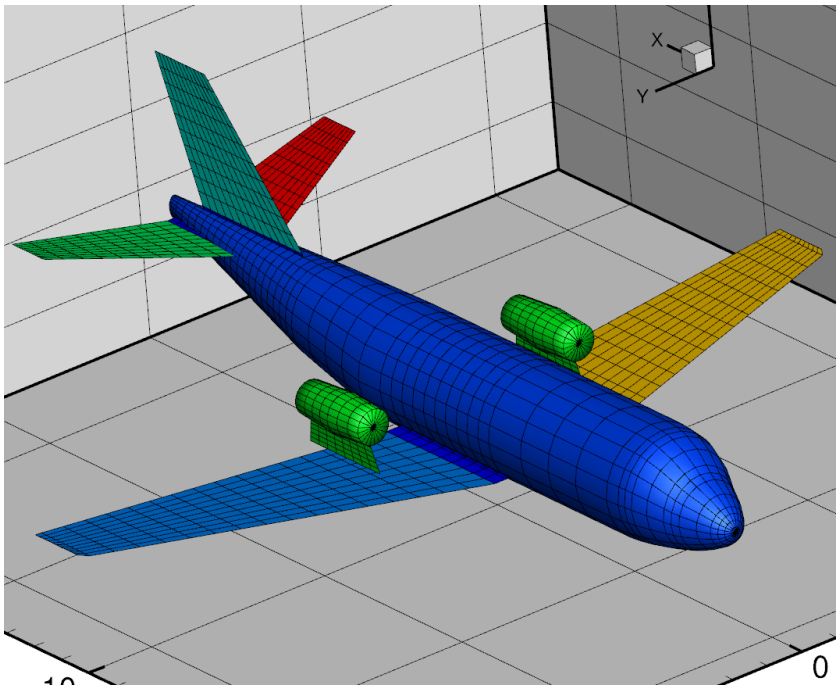

Figure 3: DLM panel model of the investigated aircraft VFW–614 ATTAS

domain. The aerodynamic model (see Fig.3) was composed of roughly 2200 DLM wing and body panels (boxes). Together with the structural eigenmodes interpolated onto the aerodynamic grid the final equation system was assembled. After a modal transformation with the 50 vacuum modes it was reduced to just this respective number of d.o.f. All aeroelastic simulations presented in this paper were conducted under ISA atmospheric conditions at sea level. The results of the flutter calculations were produced in a matched point analysis with the Ma number set to the value 0.75. A higher converged Ma number was considered to be negligible, especially for the assessment of relative differences in the flutter results.

3 THE GYROSCOPICS AND METHOD OF MODAL CORRECTION

To incorporate the engine specific terms into the aeroelastic equation of motion of the flying aeroplane the method of modal correction was applied. This approach represents an approximate solution of a system where predominant terms are to be expanded by minor terms of second order magnitude. Under the assumption of small magnitude of the correction terms the uncorrected system will be affected not significantly. Consequently the (here: real) eigenmodes, which are to be imported into the aeroelastic solver ZAERO, are still valid and represent not only the baseline but also the expanded system.

The modified homogeneous equation of motion in generalised coordinates (designated by an asterix *), where the modal correction — or rather expansion — Δ is now already incorporated, looks like:

$$(M^* + \Delta M^*)\,\ddot{q} + (D^* + \Delta D^*)\,\dot{q} + (K^* + \Delta K^*)\,q = 0 \quad . \tag{1}$$

Here the added correction matrices also have been transferred by the modal matrix Φ into

Frequencies of the VFW-614-ATTAS Baseline					
No.	f [Hz]	No.	f [Hz]	No.	f [Hz]
1	2.156855E-05	18	1.141647E+01	35	2.893649E+01
2	1.302381E-05	19	1.189815E+01	36	3.020394E+01
3	9.158021E-06	20	1.274629E+01	37	3.061813E+01
4	6.842655E-06	21	1.298601E+01	38	3.120949E+01
5	3.650023E-06	22	1.328508E+01	39	3.199958E+01
6	5.811006E-06	23	1.381981E+01	40	3.206783E+01
7	4.287803E+00	24	1.684834E+01	41	3.436589E+01
8	4.599055E+00	25	1.966559E+01	42	3.461675E+01
9	5.147471E+00	26	1.971711E+01	43	3.501454E+01
10	6.479654E+00	27	1.985010E+01	44	3.593797E+01
11	7.532699E+00	28	2.180533E+01	45	3.611039E+01
12	7.763589E+00	29	2.187030E+01	46	3.743619E+01
13	8.278665E+00	30	2.259168E+01	47	3.844436E+01
14	8.835718E+00	31	2.260227E+01	48	3.873064E+01
15	9.523818E+00	32	2.756589E+01	49	4.133935E+01
16	9.868007E+00	33	2.763763E+01	50	4.211150E+01
17	1.121284E+01	34	2.812273E+01		

Table 1: First 50 structural frequencies of the VFW-614-ATTAS baseline configuration

the modal space,

$$\Delta M^* = \Phi^T \Delta M \Phi \quad , \qquad \Delta D^* = \Phi^T \Delta D \Phi \quad , \qquad \Delta K^* = \Phi^T \Delta K \Phi \quad . \tag{2}$$

The modal matrix Φ contains either the full set of eigenvectors of the eigenvalue solution of the baseline system or only a subspace set, i.e. it must not be quadratic. As a "convergence" criteria it must be guaranteed only that there is a sufficient and suitable quantity of eigenmodes included to be capable of representing also the dynamic behaviour of the new, gyroscopic system. The thrust matrix is deflection proportional and counter acting as an additional, geometric stiffness, whereas the gyroscopic term is velocity proportional, being derived from the Coriolis forces (mass acceleration) which are caused by the moving of the masses within the rotating frame.

The antimetric, but linear gyroscopic matrix contains in general the gyro momenta caused by the engine rotation around both the global x-axis and (optional) other minor terms perpendicular to the major angular momentum which can arise from, for example, transmission components (to be multiplied further by the actual transmission ratios):

$$D^j_{gyr} := \Omega \begin{bmatrix} 0 & 0 & 0 & 0 & 0 & 0 \\ 0 & 0 & 0 & 0 & 0 & 0 \\ 0 & 0 & 0 & 0 & 0 & 0 \\ 0 & 0 & 0 & 0 & -n_z\Theta^j_z & +n_y\Theta^j_y \\ 0 & 0 & 0 & +n_z\Theta^j_z & 0 & -\Theta^j_x \\ 0 & 0 & 0 & -n_y\Theta^j_y & +\Theta^j_x & 0 \end{bmatrix} \equiv \Delta D^j \quad . \tag{3}$$

This matrix is energetically conservative, in contrast to the asymmetric and thus non-conservative but also linear thrust term, containing all six possible force and moment components arising from the impulse generation,

$$K^j_{geo} := \begin{bmatrix} 0 & 0 & 0 & 0 & +F^j_z & -F^j_y \\ 0 & 0 & 0 & -F^j_z & 0 & +F^j_x \\ 0 & 0 & 0 & +F^j_y & -F^j_x & 0 \\ 0 & 0 & 0 & 0 & +M^j_z & -M^j_y \\ 0 & 0 & 0 & -M^j_z & 0 & +M^j_x \\ 0 & 0 & 0 & +M^j_y & -M^j_x & 0 \end{bmatrix} \equiv \Delta K^j \quad , \tag{4}$$

with j being the index denominating each of the two engines. The components of these two matrices refer to the six spacial degrees of freedom of the engine reference point (c.g.; thrust point of application). Especially for the case of one single rotor the matrices get simpler with less component values. Since the engine of our example aircraft has a pitch angle of $+3°$ installation alignment here we have to take into account the rotated position additionally. The rotation about the (positive) y-axis is defined by the transformation matrix

$$T^\beta_{rot} = \begin{bmatrix} 0 & 0 & 0 & 0 & 0 & 0 \\ 0 & 0 & 0 & 0 & 0 & 0 \\ 0 & 0 & 0 & 0 & 0 & 0 \\ 0 & 0 & 0 & \cos(\beta) & 0 & +\sin(\beta) \\ 0 & 0 & 0 & 0 & 1 & 0 \\ 0 & 0 & 0 & -\sin(\beta) & 0 & \cos(\beta) \end{bmatrix} \quad . \tag{5}$$

Thus the matrices D^j_{gyr} and K^j_{geo} will be transformed into the rotated new state by

$$D^j_{gyr} \Longleftarrow T^{\beta T}_{rot} D^j_{gyr} T^\beta_{rot} \tag{6}$$

and

$$K^j_{geo} \Longleftarrow T^{\beta T}_{rot} K^j_{geo} T^\beta_{rot} \quad . \tag{7}$$

For our inclinated VFW-614 case with $\beta = -3°$ ($= +3°$ pitch angle) we will get explicitly for the gyroscopic matrix,

$$D^j_{gyr} := \Omega \begin{bmatrix} 0 & 0 & 0 & 0 & 0 & 0 \\ 0 & 0 & 0 & 0 & 0 & 0 \\ 0 & 0 & 0 & 0 & 0 & 0 \\ 0 & 0 & 0 & 0 & -\Theta^j_x \sin(\beta) & 0 \\ 0 & 0 & 0 & +\Theta^j_x \sin(\beta) & 0 & -\Theta^j_x \cos(\beta) \\ 0 & 0 & 0 & 0 & +\Theta^j_x \cos(\beta) & 0 \end{bmatrix} \equiv \Delta D^j \quad , \tag{8}$$

and the also linear but asymmetric and thus non-conservative thrust term,

$$K^j_{geo} := \begin{bmatrix} 0 & 0 & 0 & 0 & 0 & 0 \\ 0 & 0 & 0 & -F^j_x \sin(\beta) & 0 & +F^j_x \cos(\beta) \\ 0 & 0 & 0 & 0 & -F^j_x & 0 \\ 0 & 0 & 0 & 0 & 0 & 0 \\ 0 & 0 & 0 & 0 & 0 & 0 \\ 0 & 0 & 0 & 0 & 0 & 0 \end{bmatrix} \equiv \Delta K^j \quad . \tag{9}$$

4 THE FLUTTER BEHAVIOUR OF THE BASELINE CASE

As a first step the baseline configuration had been investigated. In this case the engines were taken into account as if being in a non-rotating state, i.e. they contributed to the aeroelastic aircraft model "only" with their masses and rotational engines inertias in a rigid body sense, and, being elastically mounted, they estabilshed the respective d.o.f. Since the structure of the aeroplane is (almost) symmetric, the solution of the aeroelastic eigenvalue problem renders only eigenmodes which are either symmetric or antimetric w.r.t. the vertical center plane. Therefore in the case of the occurrence of flutter instabilities the corresponding flutter modes also show either symmetric or antimetric properties.

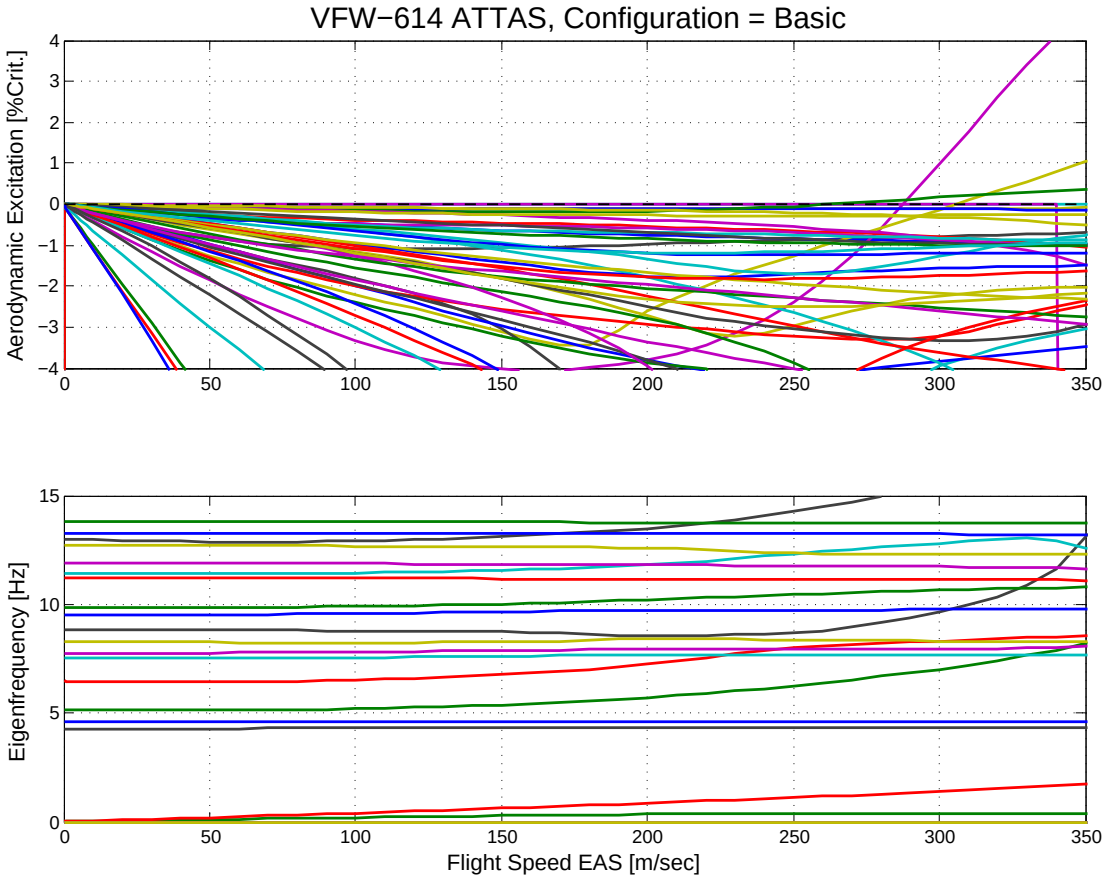

Figure 4: Flutter curves of the VFW–614 ATTAS for the *basic* configuration

In the flutter curves displaying damping and frequencies w.r.t. the flight speed (see Fig.4) there are two distinct flutter cases to be detected by the sign change of the real part of the eigenvalues from negative to positive (here displayed as aerodynamic excitation = negative aerodynamic damping, since there was no material damping allocated in the structure). The instability case with the the lower flutter speed of both is a symmetric, while the upper one is an antimetric vibration case with a predominant wing heave (for the modes see Fig.5 and 6). Prior to these two flutter cases there occurs another flutter state at the critical flight speed of around 260 [m/sec] EAS. This additional (and lowest) flutter case is of an antimetric nature with only moderate wing deflections and mainly driven by a transversal VTP motion. Since its excitation ratio is rising very moderately with the flight speed and

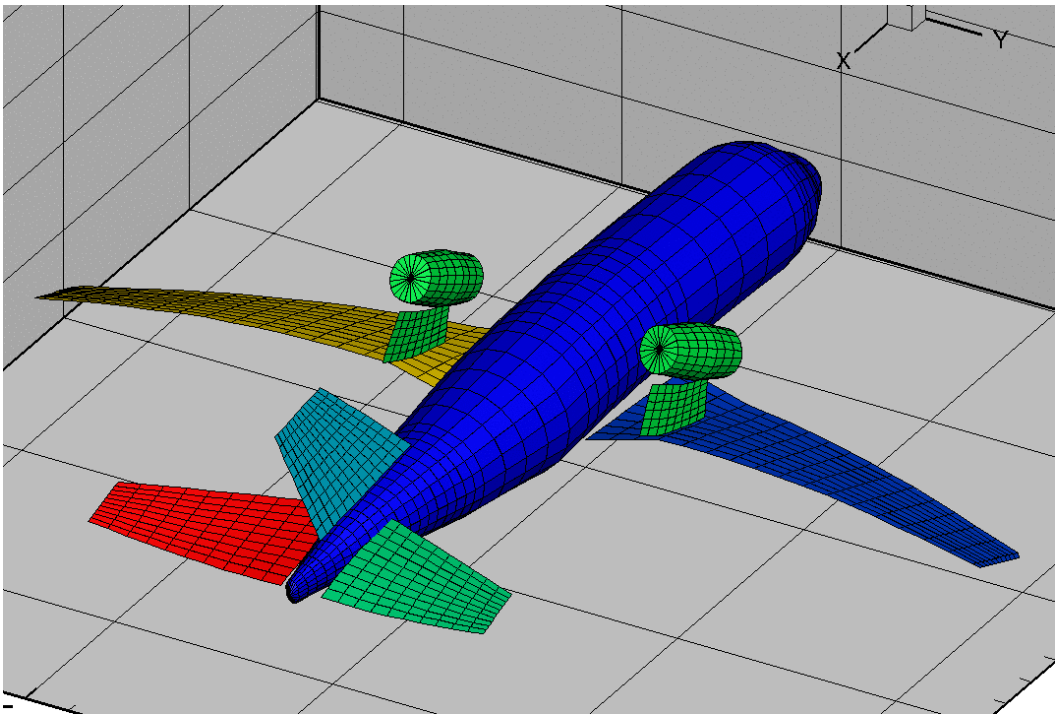

Figure 5: The symmetric flutter mode of the VFW–614 ATTAS for the *basic* configuration

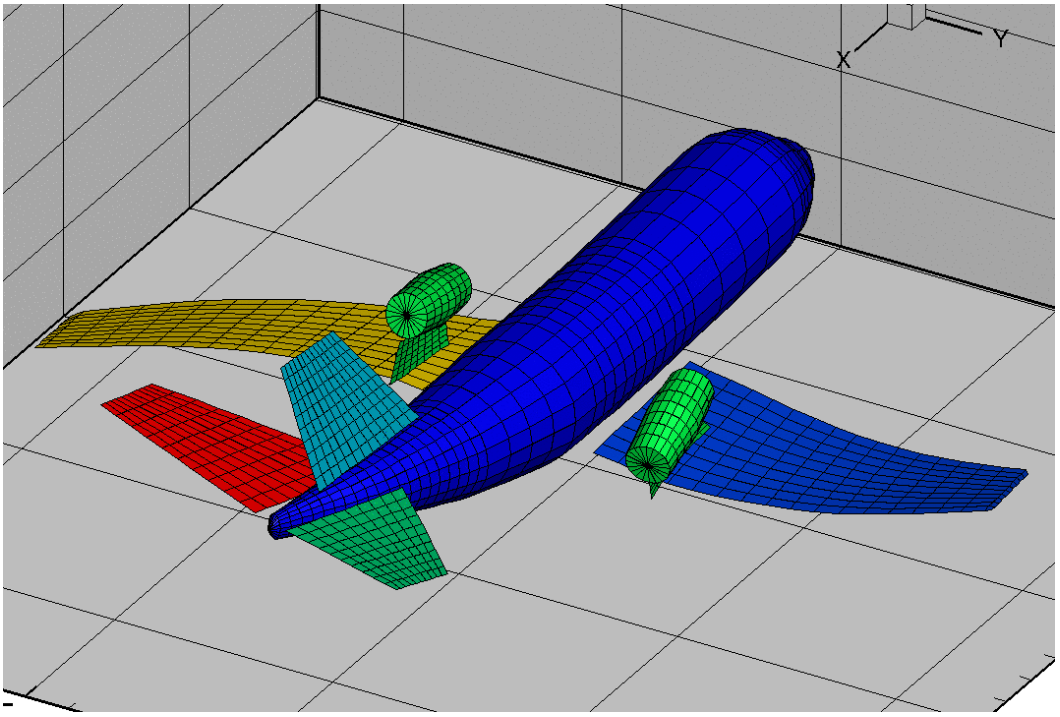

Figure 6: The antimetric flutter mode of the VFW–614 ATTAS for the *basic* configuration

because it reaches only small values ($< .5[\%]$) we ignore this flutter case in our investigation. Furthermore we can see that the respective flutter speed does not shift along with the engine modelling, which means that this flutter case is not at all affected by the pitch and yaw deflection driven gyroscopic and thrust effects. (see Fig.4, 7, 8, 9 and Tab.2).

5 THE EFFECT OF ENGINE ROTOR SPIN AND THRUST

In order to assess the impact of the added physical phenomena caused by the engines in operation on the stability behaviour of our test aeroplane there has been used a twofold procedure: The model extensions (gyroscopics, thrust force and geometrical transformation of the thrust vector) were first applied separately in an accumulated manner and then each of them compared quantitatively to the results of the baseline configuration. Both the gyroscopic moments and the force vector of the engine thrust are applied to a common grid point (FEM node) in the global coordinate system. Being attached to the wing in the rearward region of the chord the alignment of the engine axis displays an inclination angle of $+3°$ pitch. In order to incorporate this model feature, in the final engine model configuration level all engine relevant dynamical components were geometrically transformed prior to their application.

Flutter Instabilities VFW-614-ATTAS						
Flutter Mode:	Wings/"sym."		Wings/"ant."		VTP-Fuselage/ant.	
Configuration:	f [Hz]	v_∞[m/sec]	f [Hz]	v_∞[m/sec]	f [Hz]	v_∞[m/sec]
Basic	7.9238	287.49	8.3007	305.99	13.7409	263.92
Basic+Gyroscop.	7.4035 −6.6[%]	289.27 +.62[%]	7.9338 −4.4[%]	326.01 +6.5[%]	−″− 0.[%]	−″− 0.[%]
Basic+Gyroscop. +Thrust	7.4541 −5.9[%]	294.01 +2.3[%]	7.9546 −4.2[%]	321.43 +5.0[%]	−″− 0.[%]	−″− 0.[%]
Basic+Gyroscop. +Thrust+3°Inclin.	7.4021 −6.6[%]	300.68 +4.6[%]	7.9653 −4.0[%]	320.83 +4.9[%]	−″− 0.[%]	−″− 0.[%]

Table 2: The critical values of the three flutter cases of the VFW-614-ATTAS depending on the engine model configuration

The results of the eigenvalue formulation again are presented on one hand as a set of the complex eigenvalues as a function of the flight speed (frequencies and damping/excitation) and on the other hand as the corresponding eigenmodes. The eigenvalues are used to build up the flutter curves (see Fig.4, 7, 8 and 9). In the flutter analyses for all configurations of the extended engine models three flutter cases similar to those described for the baseline case and in the same order w.r.t. the flutter speed occur. The numerical values of the flutter frequencies and the flutter flight speeds for these three flutter cases and for all four engine configurations are shown Tab.2. There also the differences to the baseline case are given as the respective percentage values.

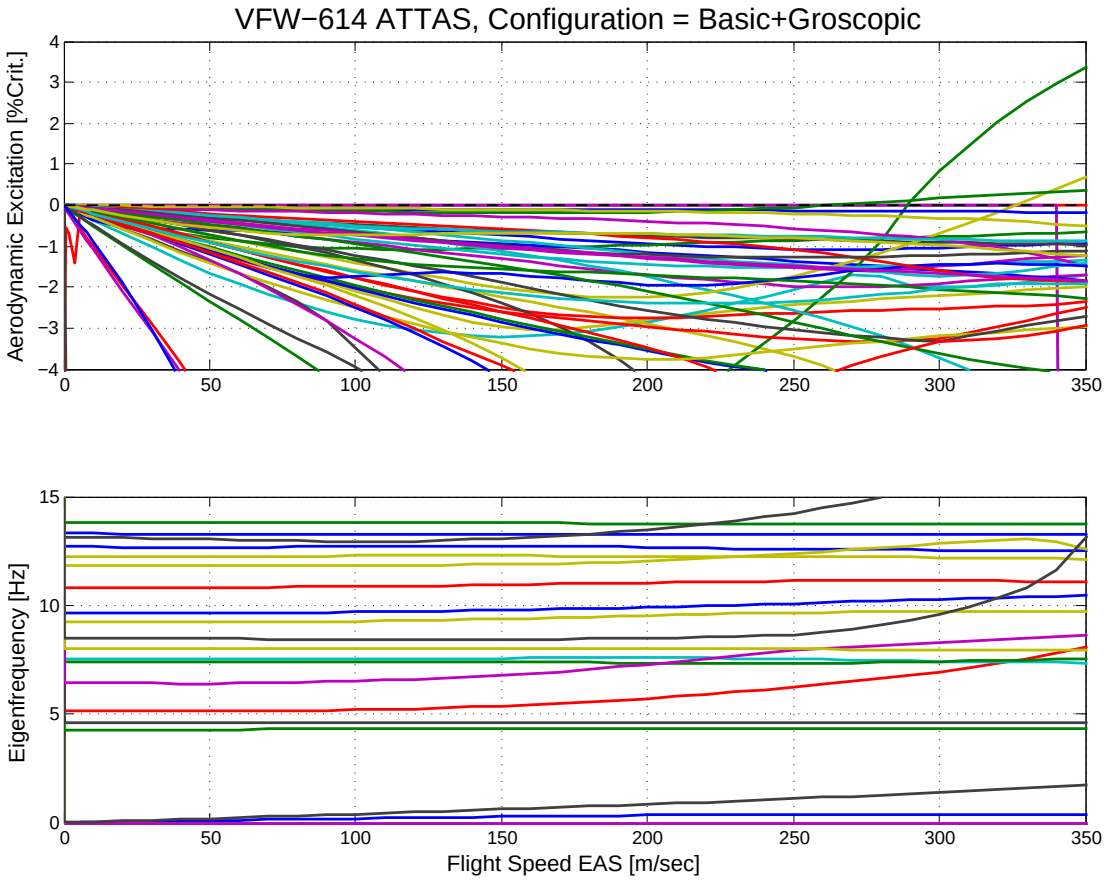

Figure 7: Flutter curves of the VFW–614 ATTAS for the *basic* configuration including engine *gyroscopics*

Both for the flutter frequencies and for the flutter flight speeds the impact of the rotating engines remains quite moderate, but with relative values up to 6[%] they should not considered to be negligible. Concerning the flutter frequencies all values are lowered which against the background of additional d.o.f. coupling caused by the gyroscopics and the follower force of the thrust appears resonable. In contrast to the frequencies all flutter flight speeds (critical speeds) here move to higher values. Since a (linear) flutter state is the result of a balance between all participating aeroelastic influences (forces), it must be stated that this drift should not be considered to be a general tendency. Instead every aeroplane configuration should be investigated individually whether the engine effects have a stabilizing impact — with their omission one would be on the conservative side —, or would lower the flutter speed thus causing a loss in stability margins.

Concerning the eigenmodes there are two flutter modes displayed for the engine baseline configuration plus gyroscopics plus thrust force to exemplify the effect of the engine model extensions visually (see Fig.10 and 11). Although the mathematical complexity is difficult to be demonstrated with only one single sketch, two snapshots of the eigenmodes have been chosen, where the symmetry breaking character of the gyroscopics is to be recognized clearly. In addition to having a highly complex phase shift in the motion of the mode components (as this is also the case in the baseline configuration) here now the symmetry features have vanished and the two flutter eigenmodes appear totally asymmetric. Nevertheless in the

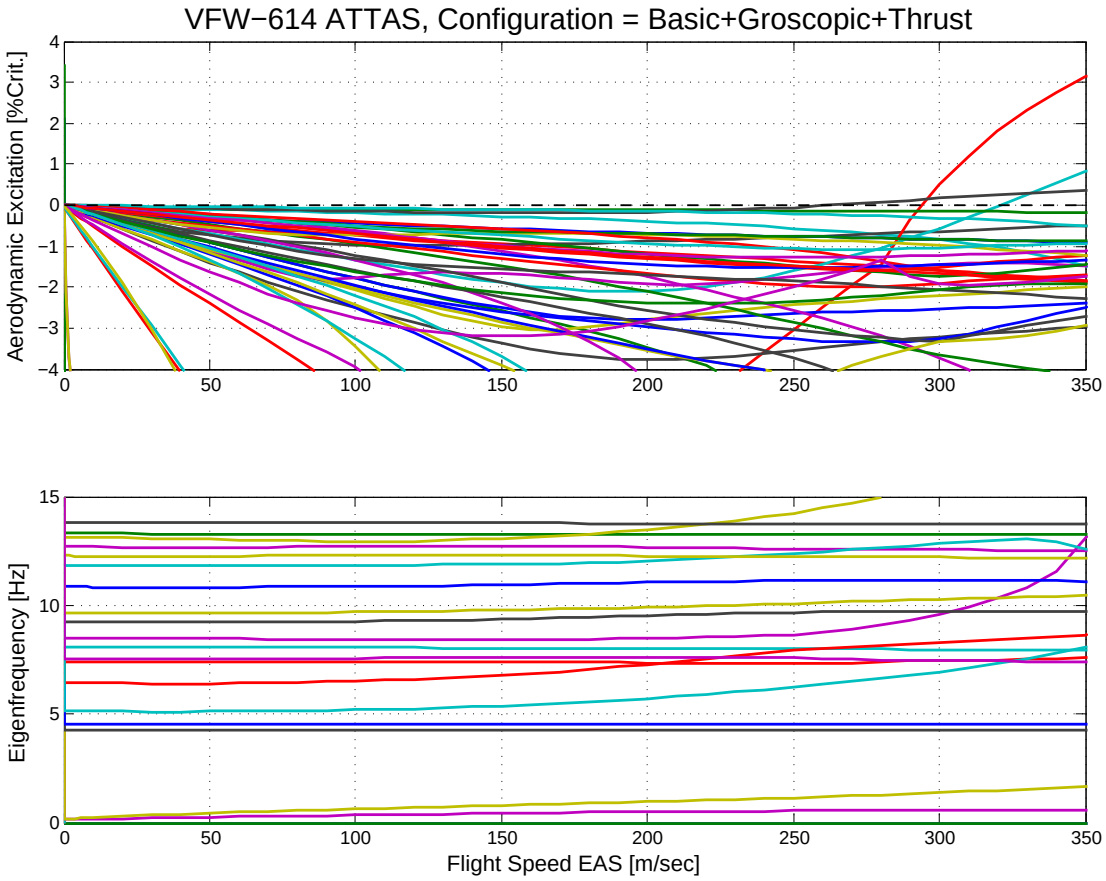

Figure 8: Flutter curves of the VFW–614 ATTAS for the *basic* configuration including engine *gyroscopics and thrust*

mode pictures (see Fig.10 and 11) and the flutter state value table Tab.2 the "symmetry classification" is maintained, but with the denomination in quotes. The practical meaning for this is to depict the corresponding modes of the baseline case as the common origin of the modified shapes and thus to be able to do a numerical comparison consecutively.

Since the dynamic extensions of the engine model are linear supplements to the (overall linear) equation of motion, by a variation of the key parameters it was tried to check roughly the "linearity" in relation to the flutter state. By assuming a linear correlation between engine thrust and the gyroscopic effect of the engine rotor (supposedly caused by the rotor speed) both phenomena were combined to one single model parameter and changed by a common factor (from 50[%] to 100[%] nominal value). In the result diagrams (see Fig.12 and 13) it is shown that the impact on the flutter frequencies could be considered approximately as linear (decreasing) whereas the impact on the flutter speed appears to be "irregularly" rising. As already mentioned above the complexity of the aeroelstic balance of the flutter state does not allow the forecast of the flutter speed in an extrapolation sense. Both sign and magnitude of the flutter speed deviation should therefore be determined in an individual and complete aeroelastic analysis.

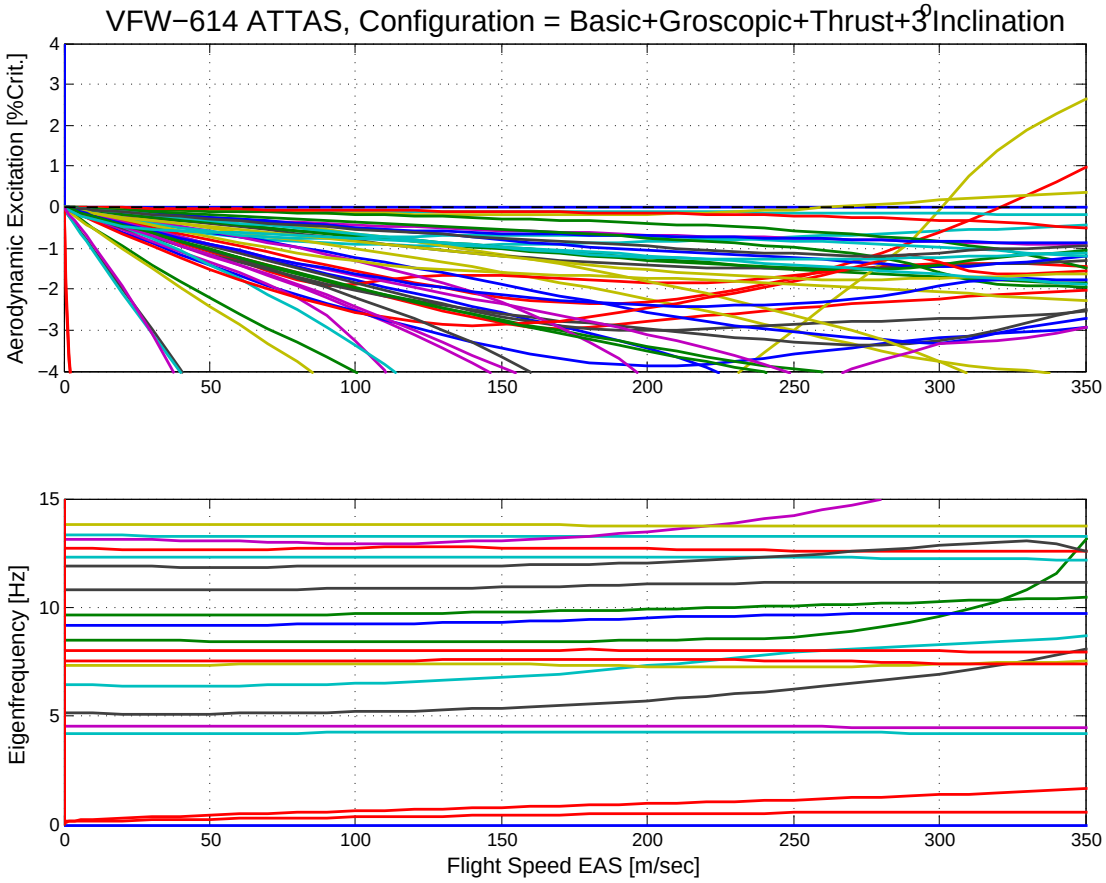

Figure 9: Flutter curves of the VFW–614 ATTAS for the *basic* configuration including engine *inclination, gyroscopics and thrust*

6 SUMMARY AND CONCLUSIONS

The objective of this research work were modelling techniques for decribing the dynamical behaviour and the structural interaction between large rotating engine masses and the fuselage of a flying aircraft. In order to take into account also the characteristics of the flexible engine-fuselage/-wing interface, specific FEM modelling features have been used. Another focus lay on the coupling of the thrust of the deflected engine (follower force) with its structural surroundings. This approach needed an enhancement and extension of the aeroelastic simulation model, which was built up by a Finite Element structural part (NASTRAN) and a Doublet Lattice aerodynamic part. The solving of the flutter equations had been executed within the aeroelastic tool ZAERO. The method of modal correction (or modal extension) was used to incorporate both the whirl and the thrust effects into the equation of motion. The linear character of the eigenvalue solution algorithm as well as the specific communication features of the aeroelastic tool ZAERO for the integration of additional engine model parameters were successfully used. As simulation platform an aeroelastic model of the 21 [to] short haul passenger jet VFW-614 ATTAS had been developed and used during the dynamic analyses. Representing the main research object in this investigation it serves as a demonstrator model as well as dynamic reference configuration for both the structural and the aerodynamic calculations.

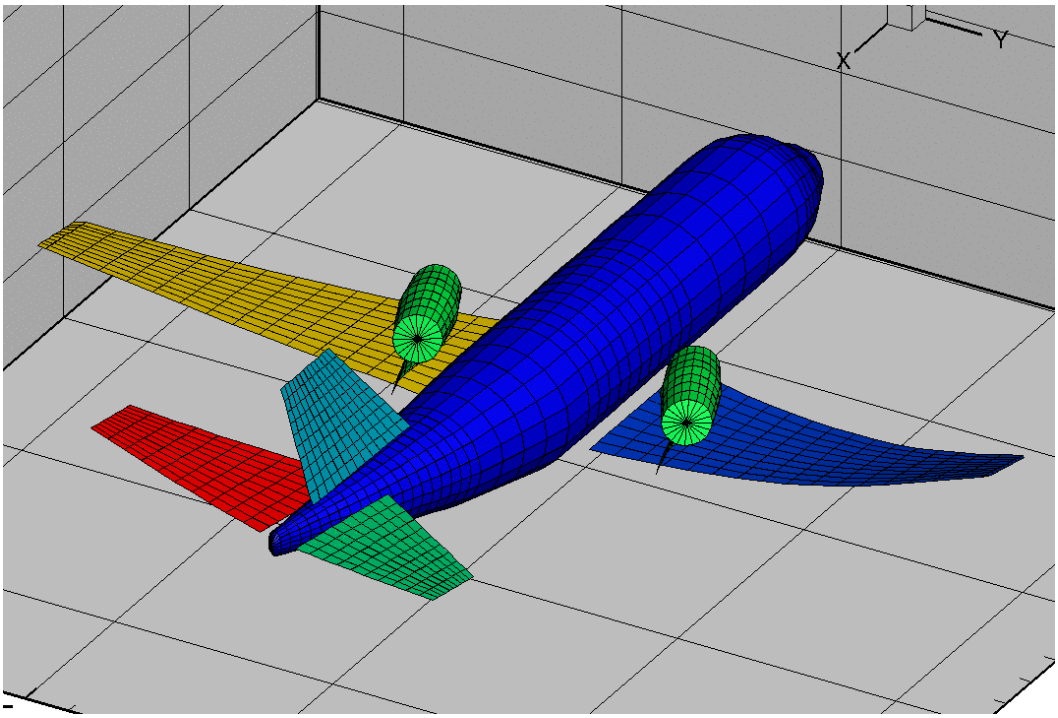

Figure 10: The "symmetric" flutter mode of the VFW–614 ATTAS for the *basic-gyroscopic-thrust* configuration

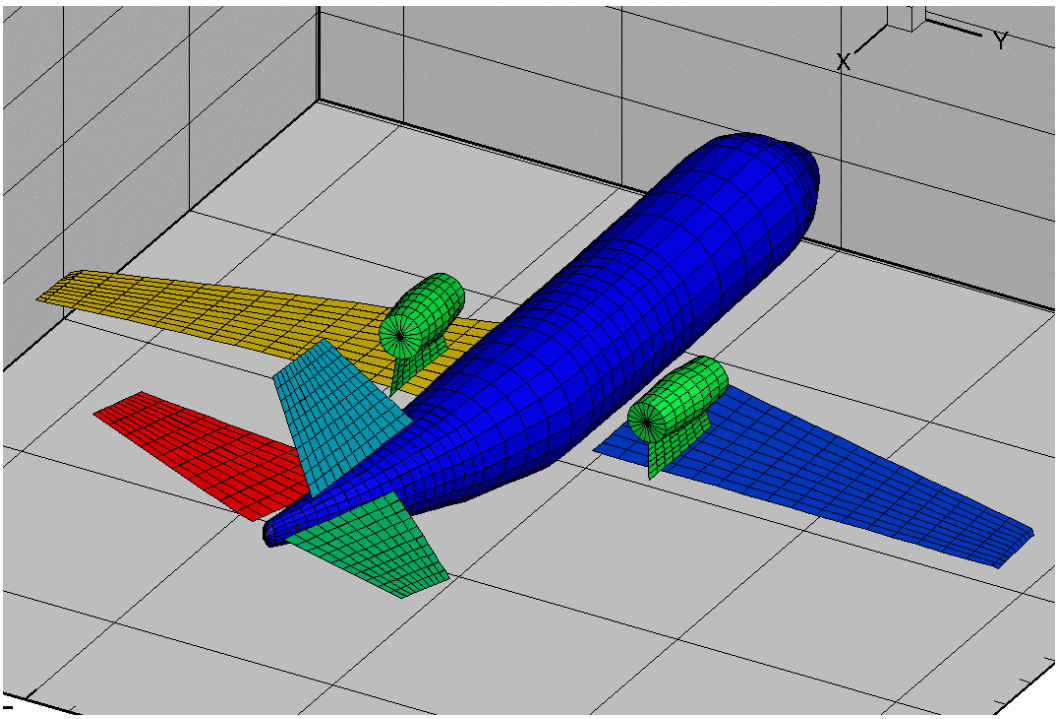

Figure 11: The "antimetric" flutter mode of the VFW–614 ATTAS for the *basic-gyroscopic-thrust* configuration

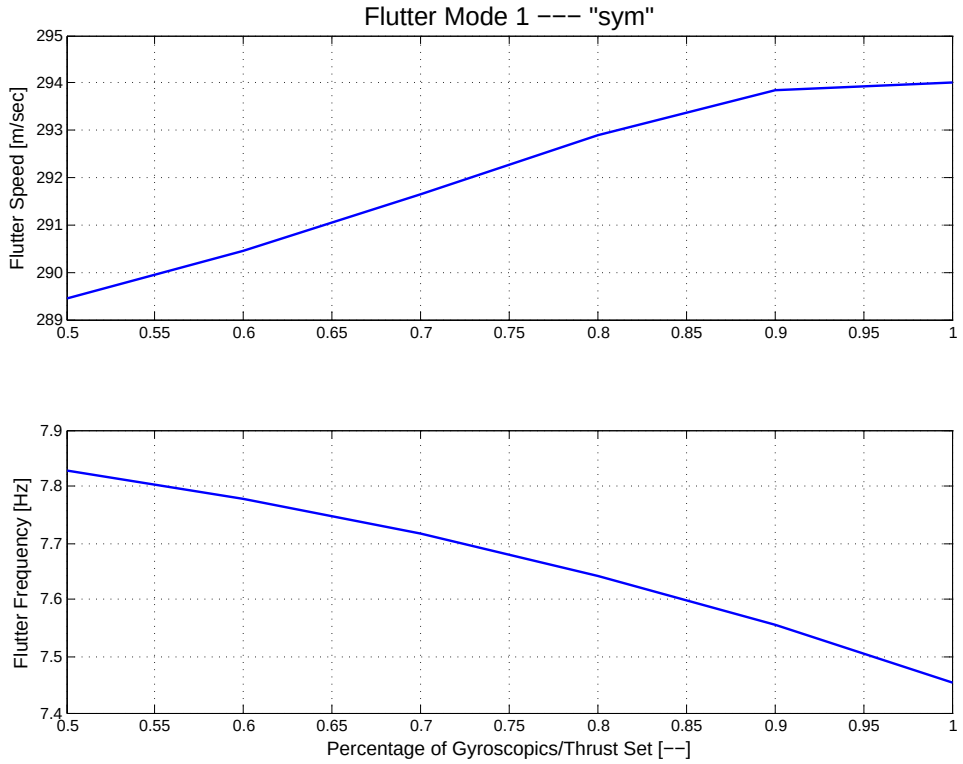

Figure 12: Flutter speed and flutter frequency of the *"symmetric"* mode in relation to the gyroscopic/thrust percentage (basic+gyroscopic+thrust)

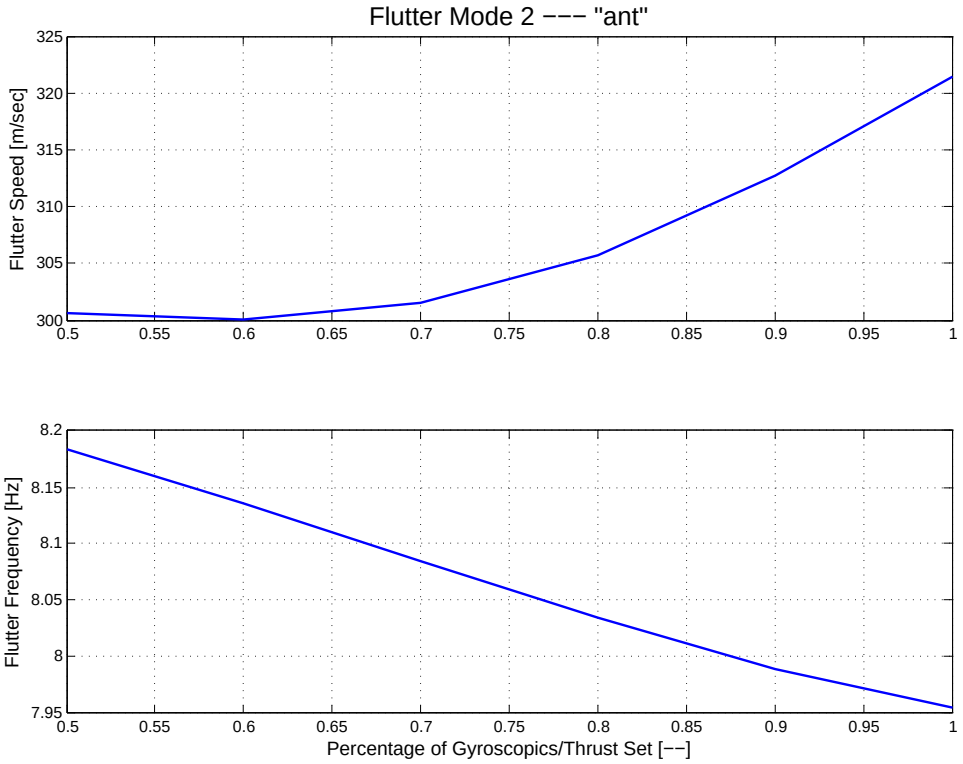

Figure 13: Flutter speed and flutter frequency of the *"antimetric"* mode in relation to the gyroscopic/thrust percentage (basic+gyroscopic+thrust)

The investigation covered modelling techniques for simulating the dynamics of the structural behaviour of the free flying aircraft in the frequency domain. In the case of the engine related terms added to the dynamical model a linearization prior to the eigenvalue analysis was required. As results of the flutter analyses the critical velocities and the flutter frequencies of the respective complex flutter eigenmodes were presented. The impact on the stability behaviour could in general be described as a softening effect in the sense of a decreasing flutter frequency, while the system became more stable by a rise of the flutter speed. Also by the variation of the engine suspension stiffness and/or the relative position of the center of gravity of the engines destabilising effects could be observed (not shown here). In any case a clear distinction between the symmetric and the antisymmetric flutter modes was no longer possible since the antisymmetric components of the gyroscopic matrix causes additional coupling of the degrees of freedom which resulted in complete asymmetric modes. Several different engine model sets have been investigated. The outcome of different parameter studies were presented as numerical results for distinct constant rotor speeds, as well as the overall dynamical behaviour w.r.t. the change of flight speed has been illustrated in flutter diagrams.

7 COPYRIGHT STATEMENT

The authors confirm that they, and/or their company or organisation, hold copyright on all of the original material included in this paper. The authors also confirm that they have obtained permission, from the copyright holder of any third party material included in this paper, to publish it as part of their paper. The authors confirm that they give permission, or have obtained permission from the copyright holder of this paper, for the publication and distribution of this paper as part of the IFASD 2015 proceedings or as individual offprints from the proceedings and for inclusion in a freely accessible web-based repository.

References

[1] Scanlan, R.H.; Truman, J.C.: *The gyroscopic effect of a rigid rotating propeller on engine and wing vibration modes.* J. Aero. Sci. 17: 653-9, 667, 1950.

[2] Savet, P.H.: *Gyroscopes: Theory and Design.* McGraw-Hill, New York, 1961.

[3] Degener, M.: *Standschwingungsversuche am Flugzeug ATD.* DLR, Institut für Aeroelastik, Göttingen, IB 232 - 98 C 05, Juli 1998.

[4] Rodden, William P.: *Theoretical and Computational Aeroelasticity.* Crest Publishing, 1^{st} Edition, 2011.

[5] Voss, Ralph, et al.: *DLR Project iGreen, Final report.* DLR, Institut für Aeroelastik, Göttingen, Februar 2012.

[6] Waitz, Stefan: *MBS Analysis of a Free Flying Helicopter with Fully Articulated Rotor.* Proc. European Rotorcraft Forum ERF2014, Southampton, 2014.

[7] Krüger, W. R.; Klimmek, T.; Liepelt, R.; Schmidt, H.; Waitz, St.; Cumnuantip, S.: *Design and aeroelastic assessment of a forward-swept wing aircraft.* CEAS Aeronautical Journal: Volume 5, Issue 4 (2014), Page 419-433, 2014.